sapphire

Sapphire Note **SP04**

High accuracy Sr isotope abundance ratio determination through Kr interference removal using the Sapphire Collision/Reaction Cell

Highlights

- Kr interferences suppression with He-O_2 cell gas mixture
- Fully mass-dependent instrumental Sr isotope fractionation
- Mean $^{87}Sr/^{86}Sr_{IC,86/88}$ = 0.710253 ± 0.000012 ($2\sigma_S$ SD; N = 80) and mean $^{84}Sr/^{86}Sr_{IC,86/88}$ = 0.056490 ± 0.000026 ($2\sigma_S$ SD; N = 80) for 16.5 ng of NIST SRM 987 Sr per individual measurement, demonstrating high measurement trueness comparable with multi-dynamic TIMS.

Radiogenic Sr isotope abundance ratios are a widely used tool in geochemistry that enables tracing mantle processes, fingerprinting sediment provenance, or reconstruction of ocean water chemistry through time (e.g., McArthur et al. 1994; Tütken et al. 2002; Krabbenhöft et al. 2009). Traditionally, Sr isotope abundance ratios have been measured on TIMS for high precision and accuracy with small sample amounts but at the expense of prolonged measurement times (Thirlwall, 1991; Charlier et al. 2006; Hans et al., 2013). Conventional MC-ICP-MS allows for fast Sr isotope abundance ratio measurements but are compromised by plasma-based interferences and high background noise. Using the Sapphire Dual Path MC-ICP-MS with Collision/Reaction Cell (CRC), interferences such as Kr can be removed using a He and O_2 gas mixture. Strontium isotope abundance ratio measurements via the CRC benefit from an improved measurement repeatability and trueness, the latter of which is comparable to multi-dynamic TIMS data (Hans et al., 2013).

Measurements were conducted in dry plasma with standard dry cones and 50 ng/ml Sr standard solutions were introduced using an Apex Omega desolvator with a 100 µl/min PFA nebulizer, corresponding to a measurand uptake rate of 0.083 ng/s. Data were acquired on Faraday cups equipped with 10^{11} Ω pre-amplifiers for an integration time of 5 s in 2 blocks of 20 acquisition cycles, equivalent to 200 s of data acquisition and consumption of 16.5 ng of Sr per measurement.

To evaluate the nature of instrumental mass bias (mass-dependent or mass-independent isotope fractionation), instrument stability, measurement trueness, and short-term repeatability, a 50 ng/ml NIST SRM 987 Sr standard solution was repeatedly (N = 80) measured over the course of 13 hours. On-peak acid blanks (2% HNO_3) were acquired for 100 s before each standard run, and each run was proceeded by a 30 s rinse and a 180 s wash in 2% HNO_3. Because tests were conducted on a pure Sr solution, no Rb interference correction was conducted.

The O_2 reactivity with Sr in the Sapphire CRC was investigated for cell gas flows of 0.4-4 ml/min of O_2. The signals of $^{88}Sr^+$ and $^{88}Sr^{16}O^+$ were thereby monitored to evaluate ion transmission and oxide formation rates. Helium was used as a collision gas to thermalize the ion beam and kept at a flow rate of 5 ml/min. The maximum sensitivity for Sr^+ species is observed for an O_2 cell gas flow of 0.7 ml/min, while SrO^+ production peaks at an O_2 cell gas flow of 1.0 ml/min with a maximum SrO^+ formation rate of 1.6 % (**Fig. 1a**). At the same time, Kr is sufficiently suppressed in the ion beam with $^{83}Kr^+$ being well within background noise compared to 8-10 mV on $^{83}Kr^+$ without the CRC (**Fig. 1b**). Notably, the background noise is also decreased by one third using the Sapphire CRC. For an O_2 cell gas flow of 0.7 ml/min and using optimised cell parameters a sensitivity of 680 V/ppm or 408 V per ng/s was achieved.

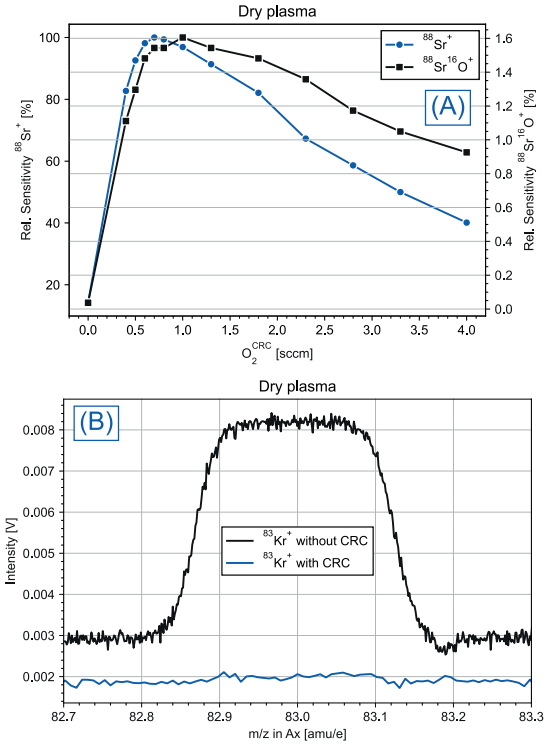

Figure 1 Oxygen reactivity with Sr for different cell gas flow rates in (**A**) and mass scan of $^{83}Kr^+$ for a 50 ng/ml Sr solution demonstrating the minimisation of residual Kr interferences and background noise in (**B**).

The preservation of mass-dependent isotope fractionation is essential for radiogenic isotope applications that utilise internal normalisation to a known stable isotope abundance ratio of the same element for correction of instrumental mass bias. In addition to mass-independent instrumental isotope fractionation, interferences can produce similar inaccuracies and apparent mass-independent isotope fractionation. While most of the Kr is removed using O_2, minor residual interferences might persist. These will be most notable on $^{84}Sr^+$, the low abundance Sr isotope with the interference of $^{84}Kr^+$, the most abundant Kr isotope. For $^{87}Sr/^{86}Sr$ and $^{86}Sr/^{88}Sr$, the residual ^{86}Kr interference is unresolvable

sapphire

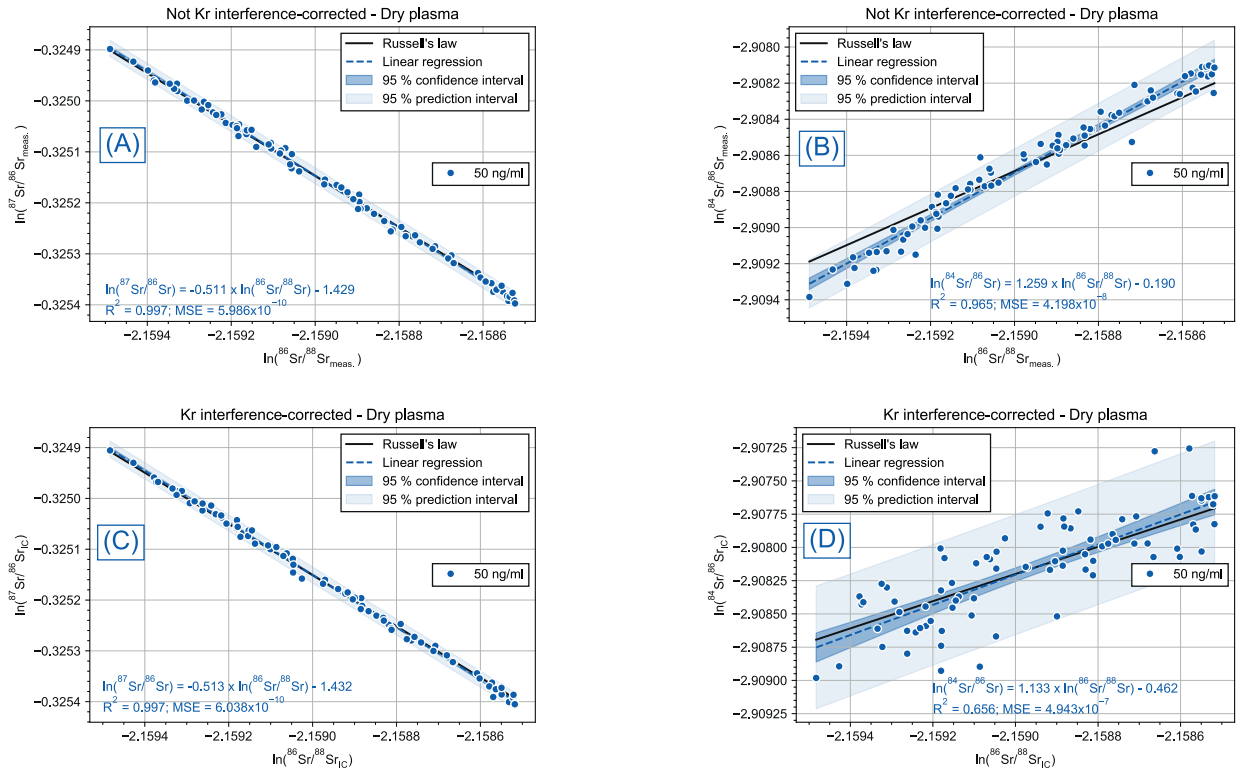

Figure 2 Instrumental isotope fractionation correlations for measured (i.e., not interference-corrected) $^{87}Sr/^{86}Sr_{meas.}$ vs. $^{86}Sr/^{88}Sr_{meas.}$ (**A**) and $^{84}Sr/^{88}Sr_{meas.}$ vs. $^{86}Sr/^{88}Sr_{meas.}$ (**B**), and for Kr interference-corrected (IC) $^{87}Sr/^{86}Sr_{IC}$ vs. $^{86}Sr/^{88}Sr_{IC}$ (**C**) and $^{84}Sr/^{88}Sr_{IC}$ vs. $^{86}Sr/^{88}Sr_{IC}$ (**D**). The black reference line indicates the theoretical fractionation line for mass-dependent isotope fractionation according to Russell's law.

from the background noise and has no significant effect on the mass-dependent isotope fractionation between $^{87}Sr/^{86}Sr_{meas.}$ vs. $^{86}Sr/^{88}Sr_{meas.}$ compared to $^{87}Sr/^{86}Sr_{IC}$ vs. $^{86}Sr/^{88}Sr_{IC}$ (**Fig. 2a, c**). For $^{84}Sr^{+}$ however, the non-interference-corrected $^{84}Sr/^{86}Sr_{meas.}$ vs. $^{86}Sr/^{88}Sr_{meas}$ deviates significantly from the mass-dependent fractionation line (**Fig. 2b**). Only after residual Kr interference correction does the empirical isotope fractionation line also follow Russell's mass-dependent fractionation law (**Fig. 2d**). Mass-independent isotope fractionation effects from the Collision/Reaction Cell itself are demonstrably insignificant.

Without residual Kr interference correction, the instrumental mass bias-corrected (internal normalisation to $^{86}Sr/^{88}Sr = 0.1194$) mean $^{87}Sr/^{86}Sr_{86/88}$ = 0.710256 ± 0.000011 ($2\sigma_S$ SD; N = 80) and $^{84}Sr/^{86}Sr_{86/88}$ = 0.056463 ± 0.000010 ($2\sigma_S$ SD; N = 80). With Kr interference correction (**Fig. 3**), the mean $^{87}Sr/^{86}Sr_{IC,86/88}$ = 0.710253 ± 0.000012 ($2\sigma_S$ SD; N = 80) and $^{84}Sr/^{86}Sr_{IC,86/88}$ = 0.056490 ± 0.000026 ($2\sigma_S$ SD; N = 80), which are both in excellent agreement with multi-dynamic TIMS data (Hans et al., 2013) of $^{87}Sr/^{86}Sr_{TIMS}$ = 0.710250 ± 0.000003 ($2\sigma_S$ SD) and $^{84}Sr/^{86}Sr_{TIMS}$ = 0.056495 ± 0.000003 ($2\sigma_S$ SD). Combined with the mass-dependent isotope fractionation, these data demonstrate that residual Kr interferences are negligible for $^{87}Sr/^{86}Sr$ abundance ratio determination. For $^{84}Sr/^{86}Sr$ however, the residual signal of the main Kr isotope ^{84}Kr can still significantly affect the accuracy of the abundance ratio and a residual Kr interference correction is beneficial. The $2\sigma_S$ SE measurement precision of individual measurements using 16.5 ng of Sr is 10-15 ppm for $^{87}Sr/^{86}Sr_{IC,86/88}$, corresponding to a mass-scaled measurement precision (see **Glossary**) of $2\sigma_s^m$ SE of 41-61 ppm^m.

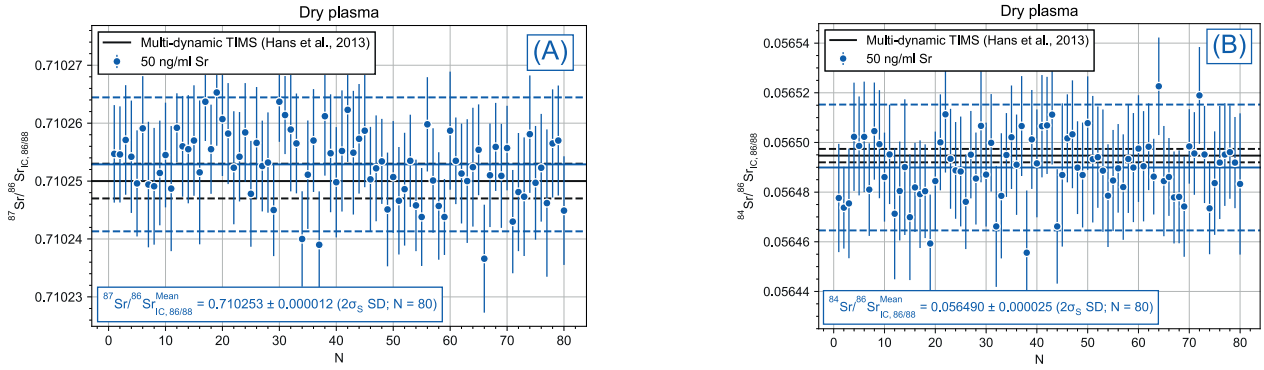

Figure 3 Residual Kr interference- and instrumental mass bias-corrected (IC,86/88; internally normalised to $^{86}Sr/^{88}Sr = 0.1194$) Sr isotope abundance ratios measured for NIST SRM 987 as (**A**) $^{87}Sr/^{86}Sr_{IC,86/88}$ and (**B**) $^{84}Sr/^{86}Sr_{IC,86/88}$. Solid and dashed lines indicate sample (S) mean ± $2\sigma_S$ SD, and error bars on the data points indicate the $2\sigma_S$ SE measurement precision of the individual measurement. High accuracy and precision multi-dynamic TIMS data from Hans et al. (2013) are added for comparison.

sapphire

The highly precise Sr isotope abundance ratio data for small sample amounts (16.5 ng) with TIMS-like measurement trueness demonstrates the effectiveness of the Sapphire Collision/Reaction Cell to remove Kr interferences and reduce background noise. Mass-dependent isotope fractionation is preserved throughout the CRC and mass-independent effects are insignificant. The Sapphire MC-ICP-MS therefore allows for fast acquisition of highly accurate and precise Sr isotope abundance ratios of small samples amounts using the Collision/Reaction Cell.

References

Charlier B.L., Ginibre C., Morgan D., Nowell G.M., Pearson D.G., Davidson J.P. & Ottley C.J. (2006). Methods for the microsampling and high-precision analysis of strontium and rubidium isotopes at single crystal scale for petrological and geochronological applications. Chemical Geology, 232(3-4), 114-133.

Hans U., Kleine T. & Bourdon B. (2013). Rb–Sr chronology of volatile depletion in differentiated protoplanets: BABI, ADOR and ALL revisited. Earth and Planetary Science Letters, 374, 204-214.

Krabbenhöft A., Fietzke J., Eisenhauer A., Liebetrau V., Böhm F. & Vollstaedt H. (2009). Determination of radiogenic and stable strontium isotope ratios ($^{87}Sr/^{86}Sr$; $\delta^{88/86}Sr$) by thermal ionization mass spectrometry applying an $^{87}Sr/^{84}Sr$ double spike. Journal of Analytical Atomic Spectrometry, 24(9), 1267-1271.

McArthur J.M. (1994). Recent trends in strontium isotope stratigraphy. Terra nova, 6(4), 331-358.

Thirlwall M.F. (1991). Long-term reproducibility of multicollector Sr and Nd isotope ratio analysis. Chemical Geology, 94(2), 85-104.

Tütken T., Eisenhauer A., Wiegand B. & Hansen B.T. (2002). Glacial–interglacial cycles in Sr and Nd isotopic composition of Arctic marine sediments triggered by the Svalbard/Barents Sea ice sheet. Marine Geology, 182(3-4), 351-372.